The time response of anaerobic digestion microbiome during an organic loading rate shock

G. H. R. Braz[1], N. Fernandez-Gonzalez[1*], J. M. Lema[1], M. Carballa[1]

[1] Department of Chemical Engineering, Institute of Technology, Universidade de Santiago de Compostela, Constantino Candeira s/n, 15782 Santiago de Compostela, Galicia, Spain

[*]corresponding author: nuria.fernandez@usc.es, phone: +34-881816019, fax: +34-881816702

ORCID:

G. H. R. Braz: 0000-0003-2176-6139

N. Fernandez-Gonzalez: 0000-0002-7468-9643

J. M. Lema: 0000-0001-5616-2584

M. Carballa: 0000-0002-7409-0235

Abstract

Knowledge of connections between operational conditions, process stability and microbial community dynamics is essential to enhance anaerobic digestion (AD) process efficiency and management. In this study, the detailed temporal effects of a sudden glycerol-based organic overloading on the AD microbial community and process imbalance were investigated in two replicate anaerobic digesters by a time-intensive sampling scheme. The microbial community time response to the overloading event was shorter than the shifts of reactor performance parameters. An increase in bacterial community dynamics and in the abundances of several microbial taxa, mainly within the *Firmicutes*, *Tenericutes* and *Chloroflexi* phyla and *Methanoculleus* genera, could be detected prior to any shift on the reactor operational parameters. Reactor acidification already started within the first 24h of the shock and headed the AD process to total inhibition in 72h alongside with the largest shifts on microbiome, mostly the increase of *Anaerosinus* sp. and hydrogenotrophic methanogenic *Archaea*. In sum, this work proved that AD microbial community reacts very quickly to an organic overloading and some shifts occur prior to alterations on the performance parameters. The latter is very interesting as it can be used to improve AD process management protocols.

Keywords

16S rRNA gene, *Firmicutes,* high-throughput sequencing, *Methanoculleous,* Microbial community, organic overloading, *Tenericutes,* turnover

Introduction

Anaerobic digestion (AD) of sewage sludge is a widely-used process and an attractive technique for waste stabilization and reduction, that also allows the production of valuable methane (Mata-Alvarez et al. 2000). The AD process is driven by different groups of microorganisms, mainly fermentative, syntrophic, acetogenic and methanogenic guilds, working symbiotically in a complex and highly interconnected community where relationships among microorganisms determine the successful performance of AD reactors (Demirel and Scherer 2008). Therefore, a better comprehension about the interconnections between operational conditions, process stability and community dynamics is essential to enhance AD efficiency (Shin et al. 2010), predict reactor performance (Razaviarani and Buchanan 2014) and conduct an effective management of the process (De Vrieze et al. 2016).

Given the complexity of AD microbial communities, several molecular tools have been applied to unravel the microbiota composition, structure and function under different operational conditions (Carballa et al. 2011; Beale et al. 2016). Although most studies focused only on methanogenic archaea due to its lower complexity and high sensitivity to AD perturbations (Razaviarani and Buchanan 2014), an increasing number of studies are also including the intricate bacterial community due to the higher resolution capacity of next generation sequencing approaches (Regueiro et al. 2015; De Vrieze et al. 2016). These efforts have shown that operational conditions, including changes on temperature, substrate type, pH, carbon/nitrogen ratio, hydraulic retention time (HRT) and organic loading rate (OLR), affect the stability of AD process and shape the microbial community (Abendroth et al. 2015).

Organic overloading is a frequent problem in AD process that causes volatile fatty acids (VFA) accumulation, which can lead to the inhibition of methanogenesis (Mao et al. 2015). The composition of the AD microbiome is affected by this process imbalance (Rétfalvi et al. 2011; Kleyböcker et al. 2012), although limited and contradictory results have been found. For instance, a study of the effects of sequential OLR shocks on sludge digesters observed that the microbiome became mainly enriched in *Firmicutes* phylum after the increments in OLR (Ferguson et al. 2016). In contrast, Regueiro et al. (2015), who used biodiesel waste to induce an OLR shock (from 2 to 10 g COD/ L d) in pig manure digesters, observed that the disturbance caused an increase in *Bacteriodetes* and *Actinobacteria* phyla.

Likewise, the archaeal community is altered during organic overloading events. High concentrations of VFAs activate the hydrogenotrophic methanogenesis pathway (Wirth et al. 2012) with the consequent community enrichment in hydrogenotrophic *Archaea*. However, while strict hydrogenotrophic archaea such as *Methanospirillum* and *Methanoculleus* are the dominant genera in some cases (Lerm et al. 2012; Hao et al. 2016); other studies detected high abundances of *Methanosarcina* after an OLR shock, which can perform both hydrogenotrophic and acetocastic methanogenesis (Steinberg and Regan 2011).

Time series studies allow to gain an ecological understanding of community dynamics, including their stability and response to external disturbances (Faust et al. 2015). However, to date most studies of AD microbiome during OLR perturbations were based on limited observations through a long period of time, including those works using the most advanced tools (Goux et al. 2015; Regueiro et al. 2015). Microbial communities can react very fast to increments in OLR, even in just few hours (Ferguson 2016), which makes necessary the use of detailed temporal studies of microbial community dynamics during perturbations to understand the roles of microorganisms in community resilience and resistance towards perturbations (Shade and Gilbert 2015). This knowledge of AD microbiome dynamics could be helpful to develop an active control strategy (Carballa et al. 2011) during the frequent OLR fluctuations that industrial digesters suffer.

The main goal of this work was to investigate the detailed temporal effects of controlled organic overloading events on the AD microbiome and their relationships with process imbalance. For that, 16S rRNA gene massive sequencing was applied to study the microbiome of replicated sludge digesters during a glycerol-based organic overloading shock.

Materials and methods

Experiment set-up

Replicated anaerobic continuously stirred (160 rpm, Heidolph RZR 2041) tank reactors, R1 and R2, with a working volume of 14 L were operated semi-continuously (once a day drawn-off and feeding) in mesophilic range (37ºC) with a hydraulic retention time (HRT) of 20 days. Both reactors were inoculated with approximately 15 g VSS/L of mesophilic anaerobic sludge from a Sewage Treatment

Plant (STP) digester. A mixture of primary and secondary sludge was used as feedstock. It was prepared every other week and stored at 4 °C. Biogas production was measured online (gas flow meter - μ flow - Bioprocess control) and its composition was analyzed by gas chromatography (HP5890 Series II, thermal conductivity detector, stainless steel column and helium as carrier gas) (García-Gen et al. 2015). Samples of reactor mixed liquor were taken twice a week, during the steady-state period for physical-chemical analysis. pH, total chemical oxygen demand (CODt), total solids (TS), volatile solids (VS), total and partial alkalinity (TA and PA) and total Kjeldahl nitrogen (N-TKN) were measured according to standard methods (APHA, 1998). VFAs concentrations were determined by gas chromatography using a Hewlett Packard 5890A device equipped with a flame ionization detector (García-Gen et al. 2015)

Organic overloading and sampling scheme

R1 and R2 were operated at an OLR of 2.5 g COD/L d, approximately. Once the steady-state was reached, an OLR shock was induced and maintained until the end of the experiment by increasing 4 times the feedstock concentration with glycerol residue obtained from biodiesel production. The selection of glycerol was based on the following reasons: i) it increases methanization efficiency when used as co-substrate (Fountoulakis and Manios 2009; Astals et al. 2012), and ii) it is highly available worldwide, with a production of more than 2 million tons of crude glycerol every year (Ciriminna et al. 2014). These characteristics make glycerol an attractive co-substrate for industrial scale use, but also likely to produce overloading events if its addition is not controlled. The response of AD microbiome to the shock was followed by an intensive sampling scheme. The experiment comprises three phases with different sampling frequencies (Table 1). Phase 1 started seven days before the OLR shock and biomass samples were taken twice a day (at 10 a.m. and 4 p.m.) to determine the microbiome fluctuation during steady-state operation. Phase 2 was defined as the period between the start of the OLR shock and before the changes in operational parameters (VFA, pH, TA, PA, biogas production) were detected. In this case, biomass samples were taken 4 times per day (at 10 a.m. and 1, 4, 7 p.m.). Finally, phase 3 started after changes in operational parameters were observed and lasted until the end of the experiment. Biomass was sampled 2-4 times per day (at 10 a.m. and 1-4-7 p.m.) during this phase (Table 1). Biomass samples consisted on well-homogenized 1 ml triplicated aliquots, that were stored at -80°C until the DNA extraction. VFAs, TA, PA, pH and

CODt were measured each time that biomass samples were collected while biogas production and composition were measured once a day.

Fluorescence in situ hybridization

Fluorescent *in situ* hybridization (FISH) was performed to identified active microbial populations of *Bacteria* and *Archaea* domains with probes Eub338mix and Arc915 respectively. Fresh biomass was sonicated for 1 min (SONIFIER^{TM} 150) and fixed in a paraformaldehyde solution (4%) according to procedure describe by Regueiro et al. (2012). The hybridization was performed at 46 °C during 90 min at 35 and 20 % (v/v) formamide concentration for Eub338mix and Arc915 respectively. Further details of both probes can be found in the probeBase database (http://probebase.csb.univie.ac.at/). Fluorescence signals were captured with an acquisition system (Coolsnap, Roper Sicientific Photometrics) coupled to an Axioskop 2 epifluorescence microscope (Zeiss, Germany). Image-Pro Plus v 2.00.06 software was used to semi-quantifty the hybridized cells with each probe in at least 20 microscopic fields per sample.

DNA extraction and high-throughput 16S rRNA amplicon sequencing.

Total genomic DNA was extracted from 1 mL biomass samples using the Stool DNA Isolation Kit (Norgen, Thorold, Canada), which combines bead-beating with chemical cell lysis, following the manufacturer instructions. Total DNA concentrations were quantified in a Qubit fluorometer (Thermo Fisher Scientific, Waltham, MA, USA) and checked for size integrity by standard electrophoresis. Fragments of the 16S rRNA gene were amplified for both *Bacteria* and *Archaea* domains. For *Bacteria*, the V3V4 region was amplified with the primer pair S-D-Bact-0341-b-S-17 and S-D-Bact-0785-a-A (Klindworth et al. 2013). For *Archaea*, the V2V3 region was amplified with the primer set Arch1F and Arch1R (Cruaud et al. 2014). In brief, a first polymerase chain reaction (PCR) was carried out in 25 uL volumes containing 3 ng of extracted DNA, 100 or 200 nM of each primers for bacterial or archaeal pairs respectively, and 1X Q5® High Fidelity Master Mix (New England BioLabs) that contains the Q5® High Fidelity DNA polymerase, 2mM $MgCl_2$ and 200 µM dNTPs. The following PCR conditions were used: initial denaturation at 98 ºC for 30 s, followed by 20 (*Bacteria* primers) or 22 (*Archaea* primers) consisting of denaturation (98 ºC for 10 s), annealing (20 s) and extension (72 ºC for 20 s) phases and a final extension step at 72 ºC during 2 min. The

annealing temperature was 50 and 48 ºC for bacterial and archaeal primers respectively. Next a similar PCR to add the Illumina adapters and barcodes to the amplicons was run for 15 cycles and with an annealing temperature of 60 ºC. DNA libraries were checked for size (578 ± 3 pb for *Bacteria* and 481 ± 12 pb *Archaea* amplicons) and concentration (20.4 ± 4.7 and 15.6 ± 4.8 nM for *Bacteria* and *Archaea* libraries respectively) using a Bioanalyzer (Bioanalyzer, Agilent Technologies, Santa Clara, CA, USA). After library preparation, samples were quantified by qPCR, pooled and sequenced in a MiSeq (Unidad de Genómica, Parque Científico de Madrid). Paired-end reads (2 × 300) were generated according to the manufacturer instructions (Illumina, Inc.).

Computational and statistical analysis

The obtained sequence reads were de-multiplexed and trimmed to remove Illumina adapters, barcodes, primers and the last 50 pb on the 5' ends due to the low-quality scores of those nucleotides (Q < 30). Then, paired reads were merged as previously described (Eren et al. 2013) enforcing the Q30 quality check and a minimum overlapping size of 50 basepairs. All sequences containing positions in which the base could not determine by the sequencer were removed from the analysis. The obtained 1.2 M bacterial and 400 K archaeal high-quality sequences were analyzed for chimera removal with VSEARCH in *de novo* mode (Rognes et al. 2016) and clustered using an open-reference approach into Operational Taxonomic Units (OTUs) at a 97% cutoff for sequence similarity in the QIIME pipeline (Caporaso et al. 2010). The taxonomic affiliation was done with USEARCH (Edgar 2010) against the Greengenes database version 13 8 (DeSantis et al. 2006). A total of 23,099 *Bacteria* and 378 *Archaea* OTUs were obtained (Online Resource –Table S1). OTUs were considered abundant if the relative abundance was larger than 1% in at least one sample.

Richness (number of distinct OTUs) and Simpson evenness (E) index that measures the equitability between the different species present in a community, were calculated based on the microbial community results. The index of resistance (Orwin and Wardle 2004; Shade et al. 2012) was determined for the richness and evenness values considering the communities in the last time point of phase 1(day 120, time 0) as the pre-perturbed reference point and the last observation of both phases 2 and 3 as the perturbed observations. To compare community structure among phases, pairwise Bray-Curtis dissimilatory matrices were calculated and represented using non-metric multidimensional scaling (NMDS). The fix window analysis was calculated using the

Bray-Curtis dissimilatory index between the initial time point (day 113) and the rest of sampling points while the moving window profile was calculated between two consecutive sampling points (Marzorati et al. 2008; Read et al. 2011). The OTUs that were differentially present between the operational phases, were identify following the DESeq2 standard differential expression analysis described by Love et al. (2014) with the default parameters. Significance was assessed by a Wald test with an alpha cutoff of 0.01.

The influence of operational parameters on the bacterial and archaeal communities diversity was analyzed using transformed-based Principal Component Analysis (tbPCA) (Legendre and Gallagher 2001) and correlation analysis (Pearson). The significance test for tbPCA was carried out by Bonferroni correction (999 permutations) and results were considered significant at a ρ-value < 0.01. The variance analysis for replicated reactors and operational results were performed with T test, considering ρ-value ≤ 0.05. Statistical and correlation analysis were performed using the R statistical environment (R Core Team 2016) with the Vegan (Oksanen et al. 2018), Phyloseq (McMurdie and Holmes 2013) and Rhea (Lagkouvardos et al. 2017) packages.

Data accessibility

The raw sequences have been deposited in the National Center for Biotechnology Information Sequence Read Archive database (SRA ID: SRP131847, BioProject ID: PRJNA432142).

Results

Anaerobic reactor performance

During phase 1 before the overloading period. In it, R1 and R2 were operated in steady-state at an OLR of 2.6 ± 0.2 g COD/ L d and none of the measured working parameters showed significant differences between the replicated reactors (ρ<0.05). CH_4 production was 0.90±0.9 g COD/ L d (Fig. 1b), corresponding to a methanization efficiency of 35±0.03 %. VFA concentration remained below 0.04 g/L (Fig. 1a) and the average content of ammonium, TS and VS were 1.7±0.05 g N/L, 52±2 g/L and 15±0.3 g/L (data not shown), respectively. These results were similar to the averaged values obtained for the initial 119 days of operation that ended alongside phase 1 (Table 2).

On day 120, the OLR was suddenly increased to 10.8 g COD/L d with glycerol to induce an organic overload initiating the phase 2. Nine hours after the shock, no significant changes in the operational parameters were observed (Fig. 1a and 1b), although methane production did not augment accordingly with the OLR (Fig. 1b).

Phase 3 started 15 hours after OLR shock once biogas rate began to increase substantially, reaching a value up to 1.5 L/L h at hour 22 (Fig. 2). In addition, biogas composition changed dramatically from 60% CH_4 and 30% CO_2 in phase 1 to 18% CH_4 and 73% CO_2 in phase 3 (Fig. 2). VFA accumulation was detected 24 hours after the OLR shock (Fig. 1a), especially propionic acid, causing the acidification of both reactors and the decrease of CH_4 production that dropped to 0.3 g COD/L d at 48 h (Fig.1b). By the end of the experiment, PA was completely consumed (Fig. 1a), pH reached low values (5.0, Fig. 1a), biogas production was almost zero (Fig. 1b and 2), methane content in the biogas was 29% (Fig. 2) and the concentrations of acetic, propionic and butyric acids were 0.53 g/L, 4.8 g/L and 0.76 g/L, respectively. Despite the changes observed in some operational parameters, VS levels in the reactors remained stable throughout the experimental period with an average of 14.0 ± 0.6 g VS/L.

Microbial community resistance and dynamics during OLR shock

Changes in community diversity indices were used to measure overall community robustness to disturbance. For that, the loss or gain of species (richness) and the changes in equitability of taxa (evenness) were analyzed. Both measurements were similar between R1 and R2 (Richness, *Bacteria*: T=1.502, ρ=0.140; *Archaea* T= -1.391, ρ =46.8. Evenness, *Bacteria*: T=-0.163, ρ=0.871; *Archaea*: T=1.701, ρ=0.095). Neither *Bacteria* nor *Archaea* richness changed after the OLR shock (Online Resource – Fig. S1). In contrast, archaeal evenness increased during phase 3 indicating a trend towards a more uniform archaeal community, while bacterial evenness was not clearly affected by the shock (Online Resource – Fig. S1). This observation was corroborated by the resistance index (RS) values. RS takes values between +1 to -1 where +1 points out to no disturbance effects and lower values indicate stronger changes. As shown in Table 3, only the index of archaeal evenness resistance measured at the end of phase 3 strongly departs from +1 values.

Changes in community structure analyzed by Bray-Curtis dissimilarities showed that both bacterial and archaeal communities were very similar between replicated

reactors (Fig. 3). In both domains, microbial communities were more similar within phases than between phases, indicating changes in the community structure with time. To evaluate those temporal changes, microbial community dynamics were calculated by means of fixed and moving window analysis of the Bray-Curtis dissimilarity index (Table 4 and Online Resource – Fig. S2). In phase 1, fixed and moving window values were nearly constant in *Bacteria* and *Archaea* communities. In contrast, the temporal change of communities accelerated during the next phases. In *Bacteria*, the moving window dynamics values incremented during phase 2 and remained constant in phase 3, while fixed window increased among phases. *Archaea,* in contrast, showed significant increments of dynamic values only during phase 3.

Microbial community composition

Replicated reactors developed similar bacterial and archaeal populations. The mean ratio of *Bacteria/Archaea* was semi-quantified by FISH. The values obtained were 2.5 ± 0.18, 2.9 ± 0.33 and 3.7 ± 0.4 for phase 1, 2 and 3, respectively. However, these values were not statistically different ($\rho \leq 0.05$) (Online Resource – Fig. S3). At phylum level, the bacterial community during phases 1 and 2 was composed mostly by *Bacteroidetes* (42%) and *Firmicutes* (18%) followed by *Cloacimonetes*, *Candidate* Division SR1 and *Proteobacteria* (Fig. 4a). The most abundant family was *Rikenellaceae* with a relative abundance of 21 % (Fig. 4b). Changes in the relative abundance of some taxonomic groups were observed when comparing the data between phases 1 and 2. For instance, *Tenericutes* phylum and the families *Erysipelotrichaceae* and *Acholeplasmatacea* increased, while *Chloroflexi* phylum, in particular *Anaerolineaceae* family, decreased. During phase 3, *Firmicutes* increased to 29 %, while *Bacteroidetes* dropped to 37 %. *Veillonellaceae* family had the biggest increase in relative abundance across all bacterial taxonomic groups, changing from $1 \cdot 10^{-4}$ %in phases 1 and 2 to 11 % in phase 3. C*lostridiaceae* 1 also flourished 48 h after the OLR shock. However, *Candidate* division SR1 and *Proteobacteria phyla* and *Ruminococcaceae* family had similar relative abundances during phases 1 and 2 (6%) but dropped in phase 3 (3 %) (Fig. 4b). The changes of these large groups were mostly driven by shifts of certain genera such as *Longilinea*, *Anaerosinus*, *Clostridium* or *Smithella* (Online Resource – Fig. S4).

The archaeal community was composed mostly by *Thermoplasmata* (WCHA1-57) class, *Methanosarcinales* family, *Methanosaeta* and *Methanoculleus* genera, which

together reached 70% in relative abundance during phases 1 and 2. 3 hours after OLR shock (phase 2), an increase in both *Woesearchaeata phylum* (from 4 to 6%) and *Methanoculleus* genera (from 2 to 5%) was observed. This trend was maintained and, in phase 3, both *Archaea* became the most relatively abundant microorganisms reaching 13 and 42%, respectively. On the other hand, *Methanosarcinales* family, *Thermoplasmata* class (WCHA1-57) and *Methanosaeta* genera dropped in phase 3 (Fig. 5).

Microorganisms differentially distributed among phases

The changes of the community diversity and structure are the results of the increase or decrease in specific microorganisms. To further explore the AD microbiome changes between phases, OTUs that were differentially abundant between phases, and therefore, representative of those operational conditions, were identified applying a differential analysis (DESeq2, $\alpha < 0.01$). Then, the OTUs found were classified according to their temporal behavior between phases. This approach allows to identify those microorganisms that quickly and consistently responded to the OLR shock.

A total of 42 *Bacteria* OTUs and 6 *Archaea* OTUs were significantly different between phase 1 to 2 ($\rho \leq 0.01$) (Online Resource – Table S2). Among them, 7 OTUs were abundant (relative abundance over 1% in any sample) (Fig. 6). For instance, *Longilinea* sp. (OTU 48579) decreased from 1.3 to 0.7%, while *Erysipelotrichaceae* UCG-004 (OTU 541244) and *Acholeplasma* (OTU 4348346) increased from 0.4 to 1.3% and from 0.8 to 1.3 %, respectively. In the archaeal community, *Methanoculleus* sp. (OTU 4323342, 1142030 and OTU NR30), *Woesearchaeota* (OTU NR63) and an uncultured *Crenoarchaea* (*Miscellaneous Crenarchaeotic* group, OTU 153278) increased in abundance (Fig. 6). From phase 2 to phase 3, the relative abundances of 32 *Bacteria* and 15 *Archaea* OTUs changed significantly (Online Resource – Table S3). The largest increase in relative abundance occurred for the *Anaerosinus* genera (OTUs 731367) and *Clostridium butyricum* sp. (OTU 238205).

Relationship between microbial community and operational parameters

The relationship between the *Bacteria* and *Archaea* community structure and the operational parameters was analyzed by tbPCA (Online Resource – Fig. S5). Both bacterial and archaeal community structures were correlated with changes in OLR, pH, methane content in the biogas, and propionate and acetate concentrations ($p \leq 0.01$). The

results indicate that OLR has some influence during *Bacteria* community changes of phase 2, but particularly during phase 3, when the largest community shifts observed are strongly correlated with the increment of OLR, the consequent increase in propionic acid and later acetic acid (days 122 and 123) and the drop of pH. Likewise, *Archaea* community structure is correlated with the same operational parameters, although in this case, the influence of both acetic and propionic acid is similar. The relationship between the operational parameters and abundant OTUs (> 1% in relative abundance in any time-point) were determined by Pearson correlations. Two profiles were found among OTUs with significant correlations ($\rho \leq 0.05$) (Fig. 7). One group of abundant OTUs had positive correlations with OLR, COD, and acetic and propionic acids and negative correlations with pH and methane content. This group includes an unknown *Bacteria* phylum, two *Firmicutes* genera and an hydrogenotrophic methanogen. In particular, *Anaerosinus* (OTUs 731367) and *Methanoculleus* (OTU 4409069) had a strong positive correlation (> 0.9) with VFAs concentration and OLR increase and a strong negative correlation with pH and CH_4 content in biogas. A second group of OTUs, that mostly include OTUs taxonomically classified as *Bacteroidetes*, presented the opposite correlations with a positive relationship with pH and CH_4 content and a negative correlation with VFAs and OLR. OTUs that changed significantly from phase 1 to 2 did not show significant correlations with any operational parameter (Fig.7).

Discussion

Better knowledge about the changes that AD microbial community suffers during organic overloading events could be key to promote an effective management of the process. In this study, the effects on the microbial community of an organic overloading event induced by adding biodiesel waste (glycerol) on replicated AD reactors were studied with a high temporal detail with the aim of expanding our understanding about the reaction of AD microbiome to that kind of events.

The microbial community assembly was similar between the replicates during the experiment, which indicates that deterministic processes have a larger role in shaping the community than stochastic processes (Zhou et al. 2013; Ju et al. 2017). Among the deterministic factors, environmental variables seem to play an important role in shaping the AD communities during the overloading. The accumulation of VFAs and consequent reactor acidification were external factors strongly affecting the

organization of the AD microbiome, as previously found (Regueiro et al. 2015; Ferguson et al. 2016).

During the steady-state operation of the reactors, the microbial communities were quite stable showing a slow temporal variability, which is characteristic of sludge communities (Shade et al. 2013). During this stage, the bacteria community profile was dominated by mainly *Bacteroidetes* but also *Firmicutes* as typically found in sewage sludge anaerobic digesters (Abendroth et al. 2015; Ferguson et al. 2016; Hao et al. 2016). The archaeal profile was more unusual as the most abundant taxon was *Thermoplasmata* WCHA1-57, an uncultured lineage for which increasing data supports its methanogenic role in anaerobic digesters (Saito et al. 2015). These dominant organisms were correlated with low OLR and neutral pH conditions suggesting their importance during the steady-state operation of the reactors.

The sudden increase in OLR resulted in a fast variation of the operational parameters in the digesters starting only 15 h after the shock with an increment in biogas production. Measurements taken 24h after overloading already indicated AD process instability, i.e.: VFAs accumulation and a large increment of biogas CO_2 concentration from 30 to 73% due to the release of CO_2 caused by the consumption of PA. Total anaerobic digestion inhibition took place after 72 h of overloading. The fast reaction of the digesters, could be explained by the high biodegradability of the glycerol used to induce the OLR shock that was likely fermented into propionate as it was the main VFA accumulated in the digesters (Viana et al. 2012). Propionate degradation under methanogenic conditions is thermodynamically less favorable than other VFAs due to the larger energy input and lower hydrogen partial pressure required (Li et al. 2012). It is well known that the different cellular yield coefficients of the microbial traits in the AD microbiome can lead to acidification as acidogenic bacteria has a faster cell growth than the acetogenic bacteria or methanogenic archaea, producing VFAs accumulation inside the reactors (Viana et al. 2012).

The AD microbial community showed early warnings of process destabilization prior to any alteration of the process parameters, such as pH or biogas production. The overall bacterial community dynamics accelerated during the first hours of overloading (phase 2). It is not surprising that bacterial populations are the first ones to react during an overloading event, as they are the responsible for the initial steps of AD process. The increment of *Acholeplasma* genus (*phylum Tenericutes*) and *Erysipelotrichaceae* family, both groups with strong positive correlations with OLR, was characteristic of

the initial 9 h of overloading. Ziganshina et al. (2015) also observed the increase in *Erysipelotrichaceae* and *Acholeplasmataceae* families during an organic overloading. Both groups, that are phylogenetically related, are mainly comprised by anaerobic species capable of fermenting glucose and other sugars to acids. Their presence in the reactors treating sewage sludge is not surprising as both taxa are associated with urogenital and gastrointestinal tracts of animals (Rosenberg et al. 2014). In this study, the addition of glycerol seems to have a positive effect in these bacteria, which might be related with a more robust cell growth and faster fermentation during the co-fermentation of sugars and glycerol than with a single substrate as has been shown for other fermentative bacteria (Wang and Yang 2013).

Although the overall archaeal community dynamics and diversity estimations did not change during phase 2, *Woesearchaeota* and *Methanoculleus* taxa significantly increased their abundances. *Methanoculleus* genera is a hydrogenotrophic methanogenic *Archaea* and a higher relative abundance of this methanogen indicates a shift towards the hydrogenotrophic pathway at the expense of the acetoclastic one (Wirth et al. 2012), which usually occurs during suboptimal operational conditions (De Vrieze et al. 2014; Ferguson et al. 2016). *Woesearchaeota* is a highly unknown new *phylum* that has been previously observed in AD communities (Tian et al. 2017), although its role is still uncertain.

Once the process parameters become altered, both *Archaea* and *Bacteria* community dynamics accelerated and large shifts in different bacterial and archaeal populations occurred. Under high OLR conditions, *Firmicutes* displaced *Bacteroidetes* as the main bacterial *phylum*, a phenomenon already reported during glycerol overloading in AD sludge reactors (Ferguson et al. 2016), although the opposite behavior was observed in pig-manure reactors (Regueiro et al. 2015). The large increment of *Firmicutes* was caused by the remarkable increase in *Anaerosinus* sp. (*Veillonellaceae* family) and *Clostridium* senso stricto 1 (*Clostridiaceae* 1 family) that occurred when high concentrations of propionic and butyric acids were detected after 24 and 48 h of overloading, respectively. *Anaerosinus* sp. are bacteria that ferments glycerol to propionate (Stömpl et al. 1999). OTUs belonging to these taxa, and to the methanogenic genera *Methanoculleus*, showed strong correlations with OLR and VFAs, highlighting the importance of these groups on community re-structuration during phases 2 and 3. The promotion of *Clostridium* species under glycerol overloading has

been detected in sludge reactors (Ferguson et al. 2016), but not in pig-manure reactors (Regueiro et al. 2015).

As already mentioned, propionate degradation during AD is difficult and it is limited to syntrophic propionate-oxidizing bacteria (SPOB). Among the four SPOB genera described, only *Smithella* was over 1 % of relative abundance in the studied reactors and it severely decreased after 48h of overloading when pH values were around 5.0. Low pH is a known factor that hinders anaerobic propionate degradation as the pH ranges for growth of all known SPOB are over 6.0 (Li et al. 2012). The inhibition of these groups could be the reason why propionic acid kept accumulating after a brief decreasing trend during the initial hours of acidification.

Archaea evenness increased in phase 3, meaning that more species become more relatively abundant in a more equitative way. Kampmann et al. (2014) already observed that the number of dominant archaea increased during overloading. During acidification, acetoclastic methanogens were displaced by hydrogenotrophic archaea, especially *Methanoculleus* sp. that considerably increased when compared to steady-state conditions. Kim et al. (2014) already detected the predominance of *Methanoculleus* sp. in AD reactors reaching unstable conditions. Previous studies have suggested that hydrogenotrophic archaea dominate communities in inhibited AD reactors due to high VFA concentrations (de Jonge et al. 2017).

Recent studies have highlighted the potential importance of the immigration of microorganisms from the feedstock on the AD microbial community dynamics overtime (Kirkegaard et al. 2017; Ju et al. 2017). However, in this work, the microbial communities of the sludge fed and the glycerol used during the shock were not analyzed and consequently, the role of the microbial community of the feed in the observed changes of AD microbiome during overloading could not be studied, what is a limitation of this work.

To conclude, this work shows in detail the short-term changes in AD microbiome during an organic overloading disturbance. It was observed that VFA accumulated within the first 24 h of shock, while methane production started to drop after 30 h. The time response of the microbial community to the OLR shock was shorter (3 h) than the changes in operational parameters (15 h). An increase in bacterial community dynamics and of the relative abundances of *Tenericutes* (*Acholeplasma*), *Erysipelotrichaceae*, *Methanoculleus* and *Woesearchaeota* were observed before any change in operational parameters occurred. Yet, the largest shifts on microbiome

occurred alongside with the operational parameters, such as the increase of *Anaerosinus* and hydrogenotrophic methanogens and the decrease of acetoclastic *Archaea*.

Acknowledgments

This research was supported by the Spanish Government (AEI) through CDTI (SmartGreenGas project, 2014-CE224). The authors belong to the Galician Competitive Research Group GRC 2013-032 and to the CRETUS Strategic Partnership (AGUP2015/02). All these programs are co-funded by FEDER (UE). PhD fellowship by CAPES (BEX-2160/2015-03) Foundation, Ministry of Education of Brazil, Brasília – DF 70040-020, Brazil. Computational resources were kindly provided and supported by *Fundacion Pública Galega Centro Tecnolóxico de Supercomputación de Galicia* (CESGA).

Compliance with ethical standards

Ethical statement

This article does not contain any studies with human participants or animals performed by any of the authors.

Conflict of interest

The authors declare that they have no conflict of interest.

References

Abendroth C, Vilanova C, Günther T, Luschnig O, Porcar M (2015) Eubacteria and Archaea communities in seven mesophile anaerobic digester plants in Germany. Biotechnol Biofuels 8:1–10. doi: 10.1186/s13068-015-0271-6

Astals S, Nolla-Ardèvol V, Mata-Alvarez J (2012) Anaerobic co-digestion of pig manure and crude glycerol at mesophilic conditions: Biogas and digestate. Bioresour Technol 110:63–70. doi: 10.1016/j.biortech.2012.01.080

Beale DJ, Karpe A V., McLeod JD, Gondalia S V., Muster TH, Othman MZ, Palombo EA, Joshi D (2016) An "omics" approach towards the characterisation of laboratory scale anaerobic digesters treating municipal sewage sludge. Water Res

88:346–357. doi: 10.1016/j.watres.2015.10.029

Caporaso JG, Kuczynski J, Stombaugh J, Bittinger K, Bushman FD, Costello EK, Fierer N, Peña AG, Goodrich JK, Gordon JI, Huttley GA, Kelley ST, Knights D, Koenig JE, Ley RE, Lozupone CA, Mcdonald D, Muegge BD, Pirrung M, Reeder J, Sevinsky JR, Turnbaugh PJ, Walters WA, Widmann J, Yatsunenko T, Zaneveld J, Knight R (2010) QIIME allows analysis of high- throughput community sequencing data. Nat Methods 7:335–336. doi: 10.1038/nmeth0510-335

Carballa M, Smits M, Etchebehere C, Boon N, Verstraete W (2011) Correlations between molecular and operational parameters in continuous lab-scale anaerobic reactors. Appl Microbiol Biotechnol 89:303–314. doi: 10.1007/s00253-010-2858-y

Ciriminna R, Pina C Della, Rossi M, Pagliaro M (2014) Understanding the glycerol market. Eur J Lipid Sci Technol 116:1432–1439. doi: 10.1002/ejlt.201400229

Cruaud P, Vigneron A, Lucchetti-Miganeh C, Ciron PE, Godfroy A, Cambon-Bonavita MA (2014) Influence of DNA extraction method, 16S rRNA targeted hypervariable regions, and sample origin on microbial diversity detected by 454 pyrosequencing in marine chemosynthetic ecosystems. Appl Environ Microbiol 80:4626–4639. doi: 10.1128/AEM.00592-14

de Jonge N, Moset V, Møller HB, Nielsen JL (2017) Microbial population dynamics in continuous anaerobic digester systems during start up, stable conditions and recovery after starvation. Bioresour Technol 232:313–320. doi: 10.1016/j.biortech.2017.02.036

De Vrieze J, Gildemyn S, Vilchez-Vargas R, Jáuregui R, Pieper DH, Verstraete W, Boon N (2014) Inoculum selection is crucial to ensure operational stability in anaerobic digestion. Appl Microbiol Biotechnol 99:189–199. doi: 10.1007/s00253-014-6046-3

De Vrieze J, Raport L, Roume H, Vilchez-Vargas R, Jáuregui R, Pieper DH, Boon N (2016) The full-scale anaerobic digestion microbiome is represented by specific marker populations. Water Res 104:101–110. doi: 10.1016/j.watres.2016.08.008

Demirel B, Scherer P (2008) The roles of acetotrophic and hydrogenotrophic methanogens during anaerobic conversion of biomass to methane: A review. Rev Environ Sci Biotechnol 7:173–190. doi: 10.1007/s11157-008-9131-1

DeSantis TZ, Hugenholtz P, Larsen N, Rojas M, Brodie EL, Keller K, Huber T, Dalevi D, Hu P, Andersen GL (2006) Greengenes, a chimera-checked 16S rRNA gene database and workbench compatible with ARB. Appl Environ Microbiol 72:5069–

5072. doi: 10.1128/AEM.03006-05

Edgar RC (2010) Search and clustering orders of magnitude faster than BLAST. Bioinformatics 26:2460–2461. doi: 10.1093/bioinformatics/btq461

Eren AM, Vineis JH, Morrison HG, Sogin ML (2013) A filtering method to generate high quality short reads using illumina paired-end technology. PLoS One 8:e66643. doi: 10.1371/journal.pone.0066643

Faust K, Lahti L, Gonze D, Vos WM De, Raes J (2015) Metagenomics meets time series analysis: unraveling microbial community dynamics. Curr Opin Microbiol 25:56–66. doi: 10.1016/j.mib.2015.04.004

Ferguson RMW, Coulon F, Villa R (2016) Organic loading rate: A promising microbial management tool in anaerobic digestion. Water Res 100:348–356. doi: 10.1016/j.watres.2016.05.009

Fountoulakis MS, Manios T (2009) Enhanced methane and hydrogen production from municipal solid waste and agro-industrial by-products co-digested with crude glycerol. Bioresour Technol 100:3043–3047. doi: 10.1016/j.biortech.2009.01.016

García-Gen S, Sousbie P, Rangaraj G, Lema JM, Rodríguez J, Steyer JP, Torrijos M (2015) Kinetic modelling of anaerobic hydrolysis of solid wastes, including disintegration processes. Waste Manag 35:96–104. doi: 10.1016/j.wasman.2014.10.012

Goux X, Calusinska M, Lemaigre S, Marynowska M, Klocke M, Udelhoven T, Benizri E, Delfosse P (2015) Microbial community dynamics in replicate anaerobic digesters exposed sequentially to increasing organic loading rate, acidosis, and process recovery. Biotechnol Biofuels 8:122. doi: 10.1186/s13068-015-0309-9

Hao L, Bize A, Conteau D, Chapleur O, Courtois S, Kroff P, Desmond-Le Quéméner E, Bouchez T, Mazéas L, Qu ED (2016) New insights into the key microbial phylotypes of anaerobic sludge digesters under different operational conditions. Water Res 102:158–169. doi: 10.1016/j.watres.2016.06.014

Ju F, Lau F, Zhang T (2017) Linking Microbial Community, Environmental Variables, and Methanogenesis in Anaerobic Biogas Digesters of Chemically Enhanced Primary Treatment Sludge. Environ Sci Technol 51:3982–3992. doi: 10.1021/acs.est.6b06344

Kampmann K, Ratering S, Geißler-Plaum R, Schmidt M, Zerr W, Schnell S (2014) Changes of the microbial population structure in an overloaded fed-batch biogas reactor digesting maize silage. Bioresour Technol 174:108–117. doi:

10.1016/j.biortech.2014.09.150

Kim S, Bae J, Choi O, Ju D, Lee J, Sung H, Park S, Sang BI, Um Y (2014) A pilot scale two-stage anaerobic digester treating food waste leachate (FWL): Performance and microbial structure analysis using pyrosequencing. Process Biochem 49:301–308. doi: 10.1016/j.procbio.2013.10.022

Kirkegaard RH, McIlroy SJ, Kristensen JM, Nierychlo M, Karst SM, Dueholm MS, Albertsen M, Nielsen PH (2017) The impact of immigration on microbial community composition in full-scale anaerobic digesters. Sci Rep 7:1–11. doi: 10.1038/s41598-017-09303-0

Kleyböcker A, Liebrich M, Verstraete W, Kraume M, Würdemann H (2012) Early warning indicators for process failure due to organic overloading by rapeseed oil in one-stage continuously stirred tank reactor, sewage sludge and waste digesters. Bioresour Technol 123:534–541. doi: 10.1016/j.biortech.2012.07.089

Klindworth A, Pruesse E, Schweer T, Peplies J, Quast C, Horn M, Glöckner FO (2013) Evaluation of general 16S ribosomal RNA gene PCR primers for classical and next-generation sequencing-based diversity studies. Nucleic Acids Res 41:1–11. doi: 10.1093/nar/gks808

Lagkouvardos I, Fischer S, Kumar N, Clavel T (2017) Rhea: a transparent and modular R pipeline for microbial profiling based on 16S rRNA gene amplicons. PeerJ 5:e2836. doi: 10.7717/peerj.2836

Legendre P, Gallagher ED (2001) Ecologically meaningful transformations for ordination of species data. Oecologia 129:271–280. doi: 10.1007/s004420100716

Lerm S, Kleyböcker A, Miethling-Graff R, Alawi M, Kasina M, Liebrich M, Würdemann H (2012) Archaeal community composition affects the function of anaerobic co-digesters in response to organic overload. Waste Manag 32:389–399. doi: 10.1016/j.wasman.2011.11.013

Li J, Ban Q, Zhang L, Jha AK (2012) Syntrophic propionate degradation in anaerobic digestion: A review. Int J Agric Biol 14:843–850.

Love MI, Huber W, Anders S (2014) Moderated estimation of fold change and dispersion for RNA-seq data with DESeq2. Genome Biol 15:1–21. doi: 10.1186/s13059-014-0550-8

Mao C, Feng Y, Wang X, Ren G (2015) Review on research achievements of biogas from anaerobic digestion. Renew Sustain Energy Rev 45:540–555. doi: 10.1016/j.rser.2015.02.032

Marzorati M, Wittebolle L, Boon N, Daffonchio D, Verstraete W (2008) How to get more out of molecular fingerprints: practical tools for microbial ecology. Environ Microbiol 10:1571–81. doi: 10.1111/j.1462-2920.2008.01572.x

Mata-Alvarez J, Macé S, Llabrés P (2000) Anaerobic digestion of organic solid wastes. An overview of research achievements and perspectives. Bioresour Technol 74:3–16.

McMurdie PJ, Holmes S (2013) Phyloseq: An R package for reproducible interactive analysis and graphics of microbiome census data. PLoS One. doi: 10.1371/journal.pone.0061217

Oksanen J, Blanchet FG, Friendly M, Kindt R, Legendre P, McGlinn D, Minchin PR, O'Hara RB, Simpson GL, Solymos P, Stevens MHH, Szoecs E, Wagner H (2018) Vegan: community ecology package. R package version 2.4-6.

Orwin KH, Wardle DA (2004) New indices for quantifying the resistance and resilience of soil biota to exogenous disturbances. Soil Biol Biochem 36:1907–1912. doi: 10.1016/j.soilbio.2004.04.036

R Core Team (2016) R: A language and environment for statistical computing. R Foundation for Statistical Computing, Vienna, Austria, Austria.

Razaviarani V, Buchanan ID (2014) Reactor performance and microbial community dynamics during anaerobic co-digestion of municipal wastewater sludge with restaurant grease waste at steady state and overloading stages. Bioresour Technol 172:232–240. doi: 10.1016/j.biortech.2014.09.046

Read S, Marzorati M, Guimarães BCM, Boon N (2011) Microbial Resource Management revisited: successful parameters and new concepts. Appl Microbiol Biotechnol 90:861–71. doi: 10.1007/s00253-011-3223-5

Regueiro L, Lema JM, Carballa M (2015) Key microbial communities steering the functioning of anaerobic digesters during hydraulic and organic overloading shocks. Bioresour Technol 197:208–216. doi: 10.1016/j.biortech.2015.08.076

Regueiro L, Veiga P, Figueroa M, Alonso-Gutierrez J, Stams AJM, Lema JM, Carballa M (2012) Relationship between microbial activity and microbial community structure in six full-scale anaerobic digesters. Microbiol Res 167:581–589. doi: 10.1016/j.micres.2012.06.002

Rétfalvi T, Tukacs-Hájos A, Albert L, Marosvölgyi B (2011) Laboratory scale examination of the effects of overloading on the anaerobic digestion by glycerol. Bioresour Technol 102:5270–5275. doi: 10.1016/j.biortech.2011.02.020

Rognes T, Flouri T, Nichols B, Quince C, Mahé F (2016) VSEARCH: a versatile open source tool for metagenomics. PeerJ 4:e2584. doi: 10.7717/peerj.2584

Saito Y, Aoki M, Hatamoto M, Yamaguchi T (2015) Presence of a novel methanogenic archaeal lineage in anaerobic digesters inferred from mcrA and 16S rRNA gene phylogenetic analyses. J Water Environ Technol 13:279–289.

Shade A, Gilbert JA (2015) Temporal patterns of rarity provide a more complete view of microbial diversity. Trends Microbiol 23:335–340. doi: 10.1016/j.tim.2015.01.007

Shade A, Gregory Caporaso J, Handelsman J, Knight R, Fierer N, Caporaso JG, Handelsman J, Knight R, Fierer N (2013) A meta-analysis of changes in bacterial and archaeal communities with time. ISME J 7:1493–1506. doi: 10.1038/ismej.2013.54

Shade A, Peter H, Allison SD, Baho DL, Berga M, Bürgmann H, Huber DH, Langenheder S, Lennon JT, Martiny JBH, Matulich KL, Schmidt TM, Handelsman J (2012) Fundamentals of microbial community resistance and resilience. Front Microbiol 3:417. doi: 10.3389/fmicb.2012.00417

Shin SG, Han G, Lim J, Lee C, Hwang S (2010) A comprehensive microbial insight into two-stage anaerobic digestion of food waste-recycling wastewater. Water Res 44:4838–4849. doi: 10.1016/j.watres.2010.07.019

Steinberg LM, Regan JM (2011) Response of lab-scale methanogenic reactors inoculated from different sources to organic loading rate shocks. Bioresour Technol 102:8790–8798. doi: 10.1016/j.biortech.2011.07.017

Tian JH, Pourcher AM, Bureau C, Peu P (2017) Cellulose accessibility and microbial community in solid state anaerobic digestion of rape straw. Bioresour Technol 223:192–201. doi: 10.1016/j.biortech.2016.10.009

Viana MB, Freitas A V., Leitão RC, Pinto GAS, Santaella ST (2012) Anaerobic digestion of crude glycerol: a review. Environ Technol Rev 1:81–92. doi: 10.1080/09593330.2012.692723

Wang Z, Yang ST (2013) Propionic acid production in glycerol/glucose co-fermentation by Propionibacterium freudenreichii subsp. shermanii. Bioresour Technol 137:116–123. doi: 10.1016/j.biortech.2013.03.012

Wirth R, Kovács E, Maróti G, Bagi Z, Rákhely G, Kovács KL (2012) Characterization of a biogas-producing microbial community by short-read next generation DNA sequencing. Biotechnol Biofuels 5:41. doi: 10.1186/1754-6834-5-41

Zhou J, Liu W, Deng Y, Jiang Y-H, Xue K, He Z, Van Nostrand JD, Wu L, Yang Y, Wang A (2013) Stochastic Assembly Leads to Alternative Communities with Distinct Functions in a Bioreactor Microbial Community. MBio 4:e00584-12-e00584-12. doi: 10.1128/mBio.00584-12

Ziganshina EE, Belostotskiy DE, Ilinskaya ON, Boulygina EA, Grigoryeva T V., Ziganshin AM (2015) Effect of the Organic Loading Rate Increase and the Presence of Zeolite on Microbial Community Composition and Process Stability During Anaerobic Digestion of Chicken Wastes. Microb Ecol 70:948–960. doi: 10.1007/s00248-015-0635-2

FIGURE CAPTIONS

Fig. 1 Reactors performance during phases 1, 2 and 3. Daily average values from R1 and R2 and standard deviation. **a)** pH, total and partial alkalinity. **b)** Accumulated CH_4 production and acetic, propionic and butyric acid concentration.

Fig. 2 Volumetric biogas production (L/L h) and biogas composition during 24 hours before and 72 hours after OLR shock in R2. Similar values were observed in R1.

Fig. 3 Non-metric multidimensional scaling (NMDS) analysis of Bray-Curtis dissimilarities for **a)** *Bacteria* and **b)** *Archaea*. Samples from the same phase are connected to their centroid. The ellipses indicate the standard deviation of distances within each cluster.

Fig. 4 Relative abundances of the most abundant *Bacteria* taxa averaged across replicated reactors: **a)** prevalent phyla, **b)** prevalent families. Samples are organized by day of the experiment (d) and hour (h) after OLR shock. For phase 1, samples are identified by the period of sampling (m = morning, a = afternoon). Only taxa exceeding 1% in average are shown in the figure; all taxa below that threshold are included in the group "Other".

Fig. 5 Relative abundances of the most abundant *Archaea* genera averaged across replicated reactors. Samples are organized by day of the experiment (d) and hour (h) after OLR shock. For phase 1, samples are identified by the period of sampling (m =

morning, a = afternoon). Only genera exceeding 1% in average are shown in the figure; all taxa below that threshold are included in the group "Other".

Fig. 6 Abundant OTUs that are differentially distributed between phases 1 and 2. For each OTU, the difference of averaged relative abundance between phases 1 and 2 is shown. Positive values indicate increments with time whereas negative values represent a decline.

Fig. 7 Pearson correlations of abundant OTUs and the operational parameters OLR, pH, acetic and propionic acid concentrations and methane content in the biogas. Only significant correlations are shown ($\rho \leq 0.05$).

Table 1. Phase characteristics and sampling scheme for monitoring the microbiome during the experiment.

	Steady-state period	**OLR shock period**	
	Phase 1	*Phase 2*	*Phase 3*
OLR (g COD/L d)	2.5 ± 0.2	10.8 ± 0.02	10.8 ± 0.02
Phase characteristic	Steady-state	No changes in operational parameter after OLR shock	operational parameter changed after OLR shock
Samples	Twice per day	4 times per day	2-4 times per day

Table 2: Anaerobic reactor working parameters along the initial 119 days of operation (average values of both reactors and standard deviations).

Parameter	Value (n = 59)
pH	7.38 ± 0.11
Total alkalinity (g $CaCO_3$/L)	3.6 ± 0.1
Partial alkalinity (g $CaCO_3$/L)	2.8 ± 0.1
Total solids (g/L)	42.1 ± 7.6
Volatile solids (g/L)	13.8 ± 1.1
Ammonium (g N/L)	1.70 ± 0.14
Acetic acid (mg/L)	< 60
Propionic acid (mg/L)	< 30
CH_4 production (g COD/L d)	0.94 ± 0.16

Table 3. Richness and evenness resistance indices for *Archaea* and *Bacteria*.

	Bacteria		***Archaea***	
Change from phase 1 to:	**phase 2**	**phase 3**	**phase 2**	**phase 3**
Richness	0.916	0.897	0.933	0.825
Evenness	0.813	0.779	0.992	0.091

Table 4. Microbial community dynamics averaged by phase and domain expressed as the percentage of community change. Moving window dynamics compares community changes between consecutive time-points, whereas fixed window dynamics compare each time point to the initial community.

	Moving window dynamics (%)		**Fixed window dynamics (%)**	
	Bacteria	*Archaea*	*Bacteria*	*Archaea*
Phase 1	50.6 ± 0.9	15.5 ± 2.4	51.4 ± 1.1	15.8 ± 2.3
Phase 2	52.4 ± 1.5	16.4 ± 2.4	53.9 ± 0.8	19.0 ± 1.9
Phase 3	52.6 ± 1.2	18.8 ± 3.0	58.0 ± 1.7	31.0 ± 9.2

Fig1

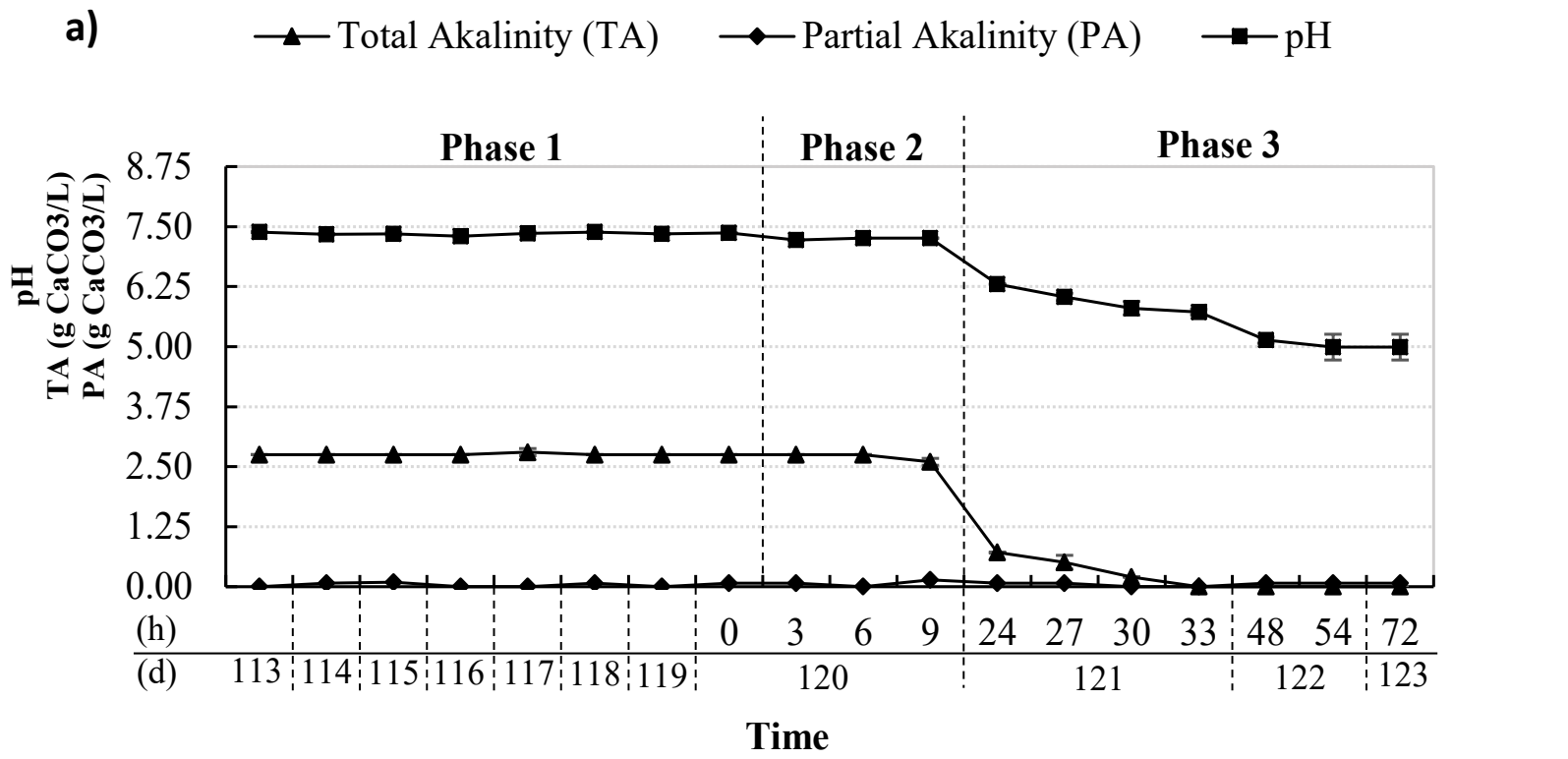
a)
Total Akalinity (TA)
Partial Akalinity (PA)
pH
Phase 1
Phase 2
Phase 3
pH
TA (g CaCO3/L)
PA (g CaCO3/L)
8.75
7.50
6.25
5.00
3.75
2.50
1.25
0.00
(h)
0 3 6 9 24 27 30 33 48 54 72
(d)
113 114 115 116 117 118 119 120 121 122 123
Time

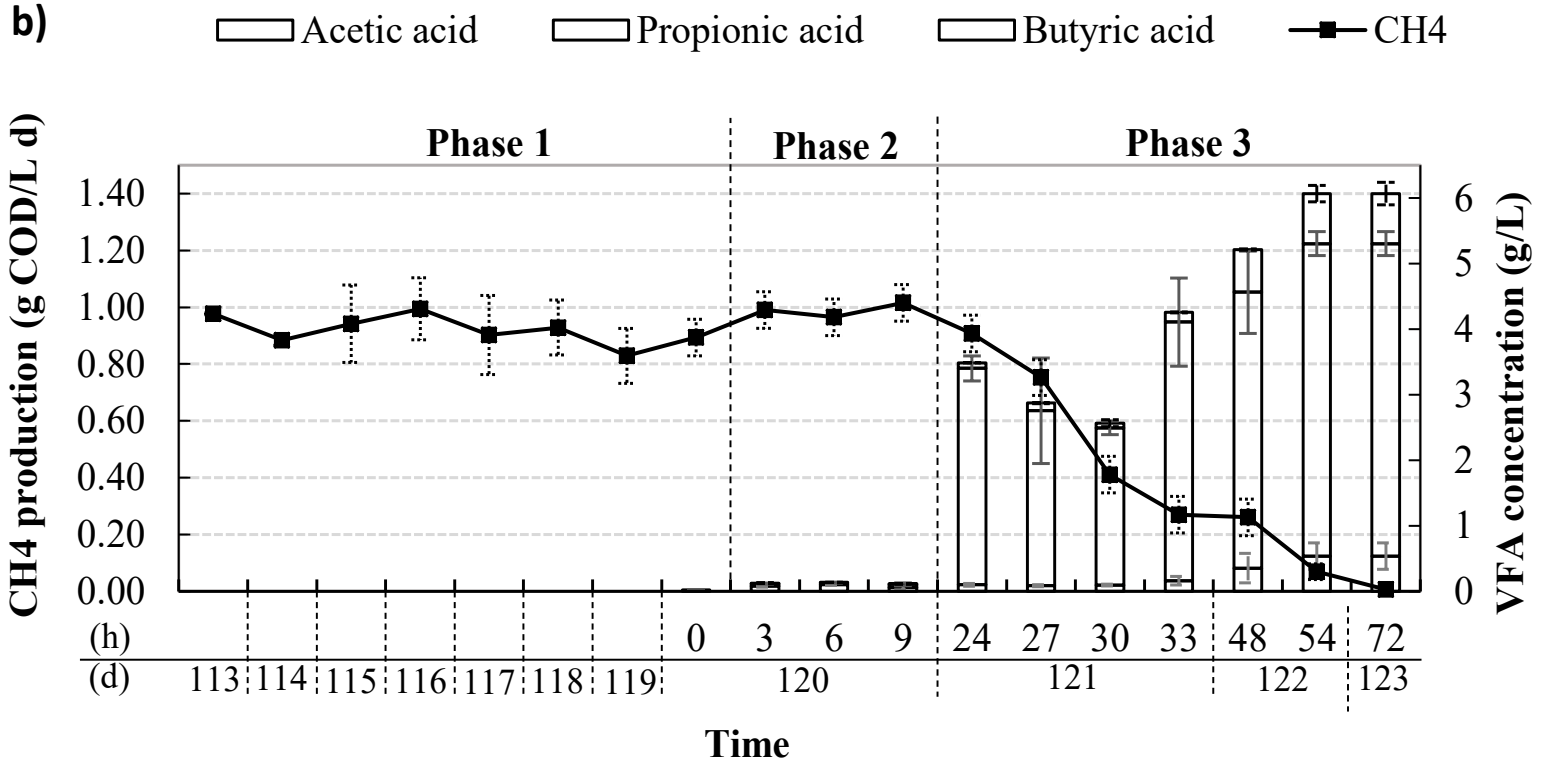
b)
Acetic acid
Propionic acid
Butyric acid
CH4
Phase 1
Phase 2
Phase 3
CH4 production (g COD/L d)
VFA concentration (g/L)
1.40
1.20
1.00
0.80
0.60
0.40
0.20
0.00
6
5
4
3
2
1
0
(h)
0 3 6 9 24 27 30 33 48 54 72
(d)
113 114 115 116 117 118 119 120 121 122 123
Time

Fig2

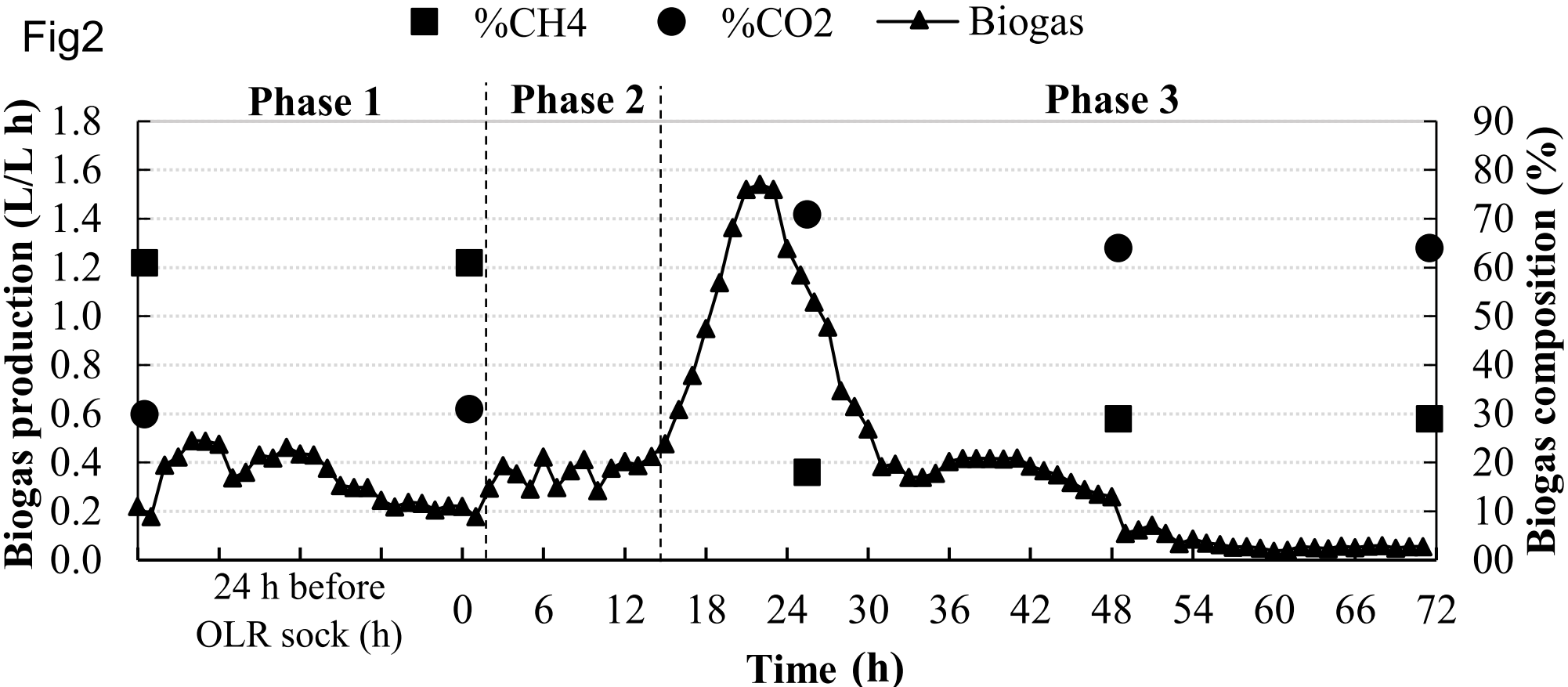
%CH4
%CO2
Biogas
Phase 1
Phase 2
Phase 3
Biogas production (L/L h)
Biogas composition (%)
1.8
1.6
1.4
1.2
1.0
0.8
0.6
0.4
0.2
0.0
90
80
70
60
50
40
30
20
10
00
24 h before OLR sock (h)
0
6
12
18
24
30
36
42
48
54
60
66
72
Time (h)

Fig3_corrected

a)

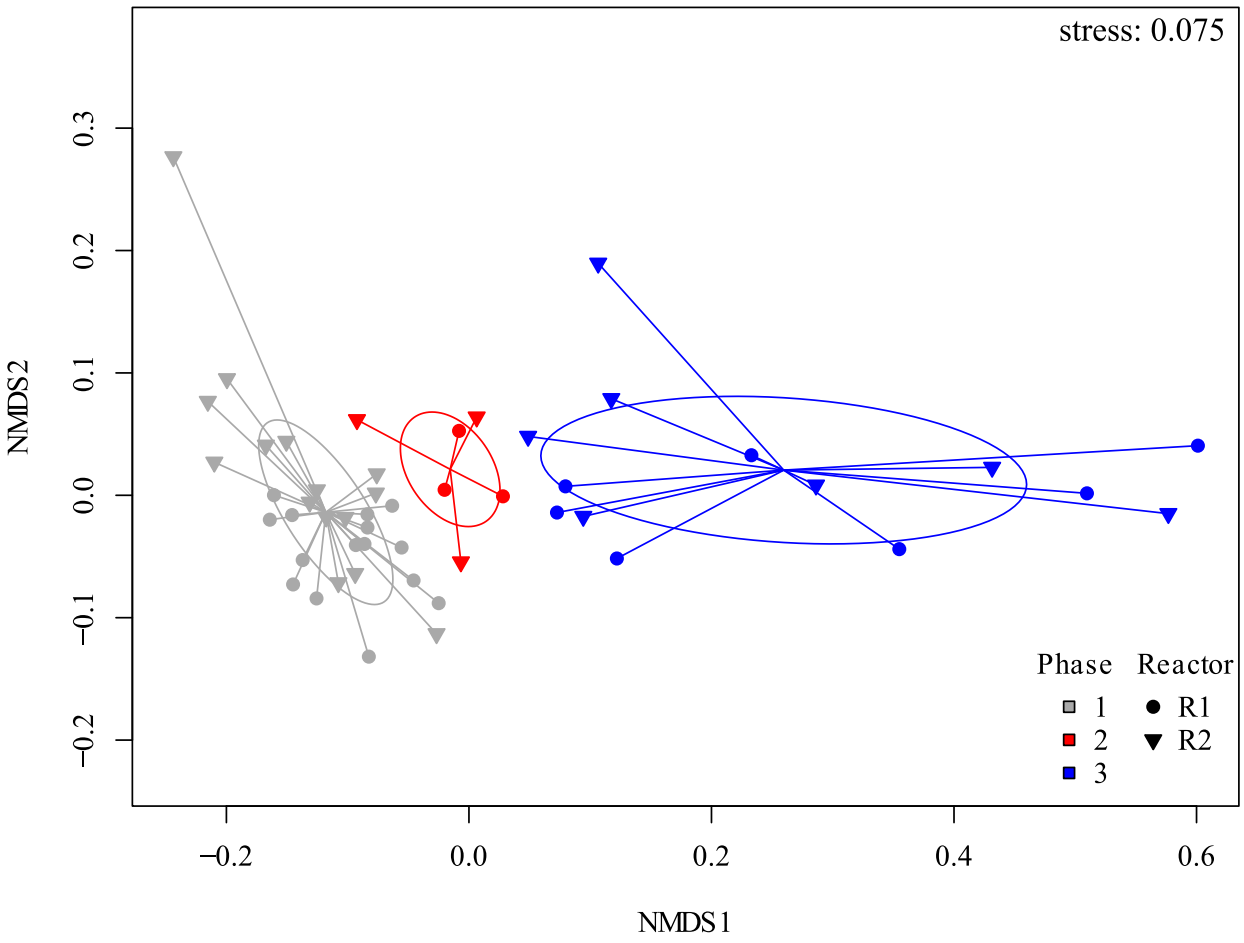

b)

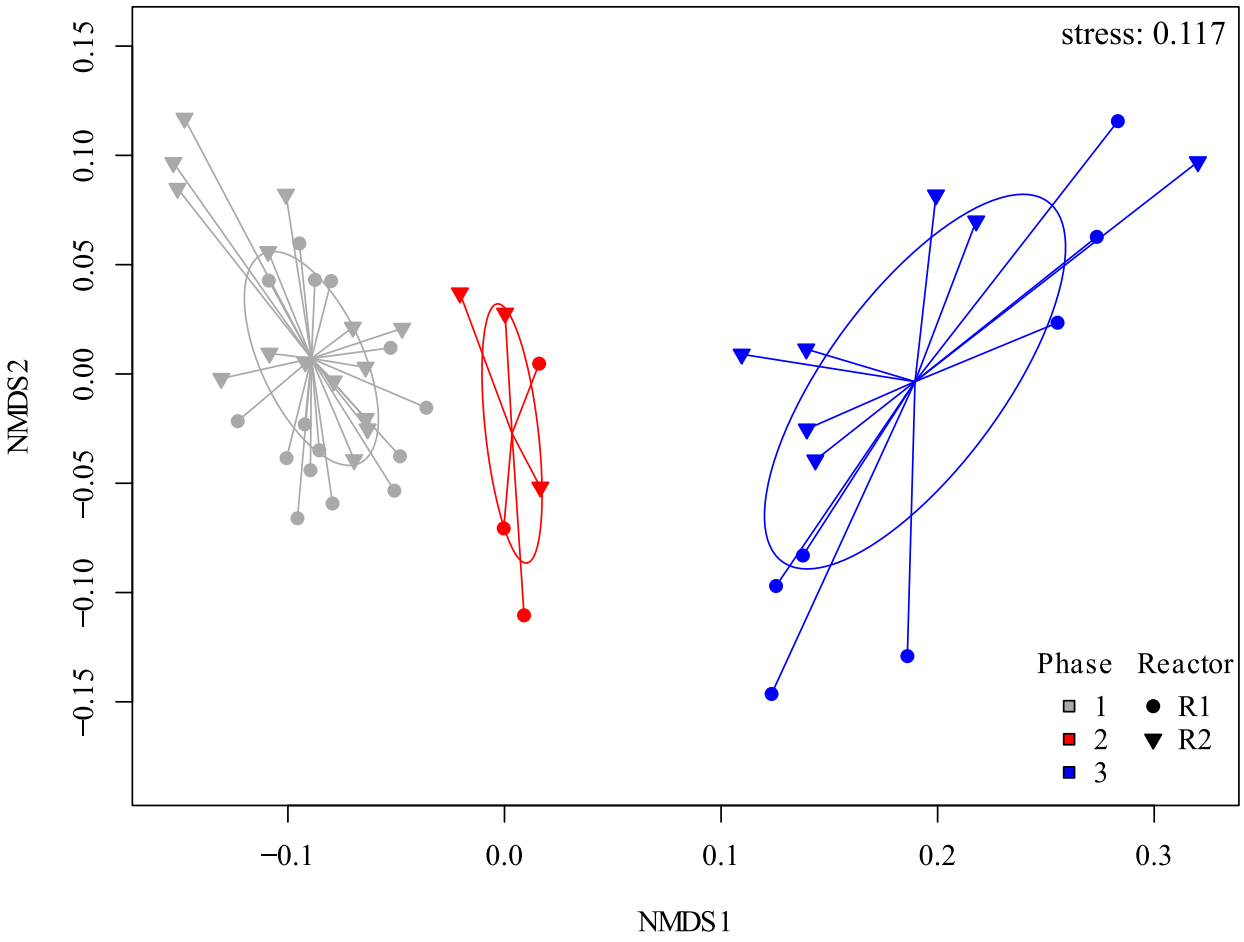

Fig 4

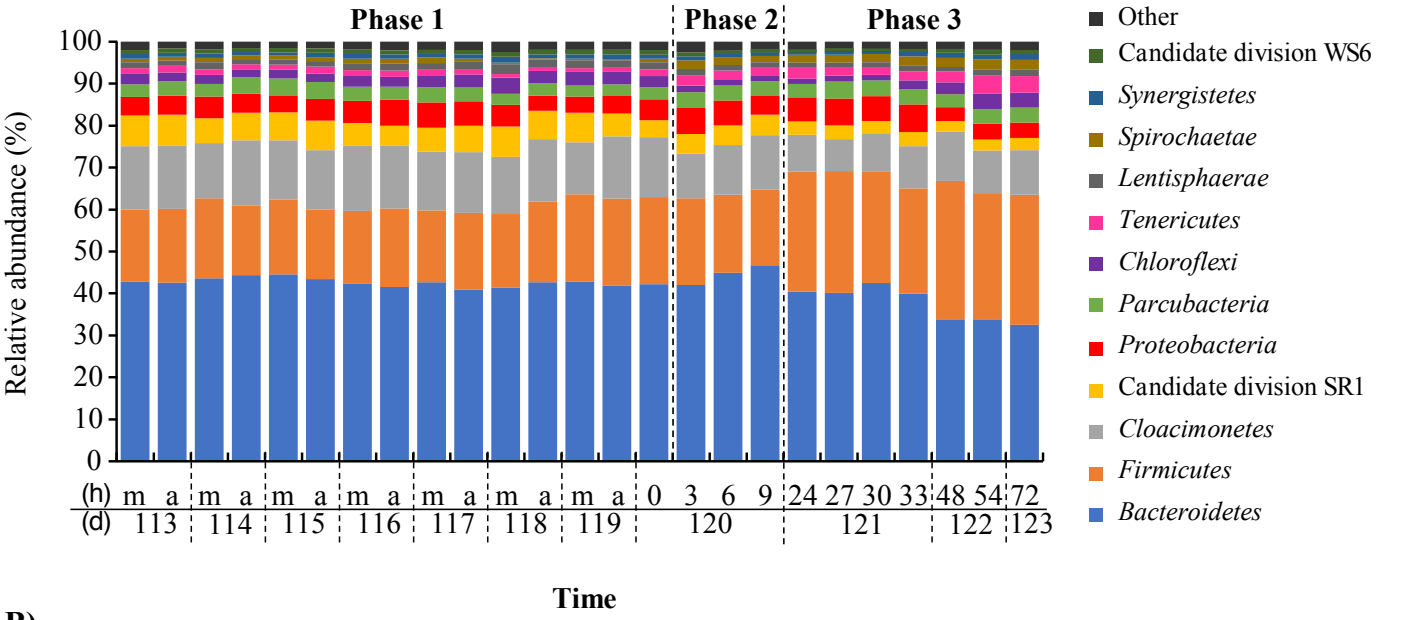
A)
Phase 1
Phase 2
Phase 3
Relative abundance (%)
100
90
80
70
60
50
40
30
20
10
0
(h) m a m a m a m a m a m a m a 0 3 6 9 24 27 30 33 48 54 72
(d) 113 114 115 116 117 118 119 120 121 122 123
Time
Other
Candidate division WS6
Synergistetes
Spirochaetae
Lentisphaerae
Tenericutes
Chloroflexi
Parcubacteria
Proteobacteria
Candidate division SR1
Cloacimonetes
Firmicutes
Bacteroidetes

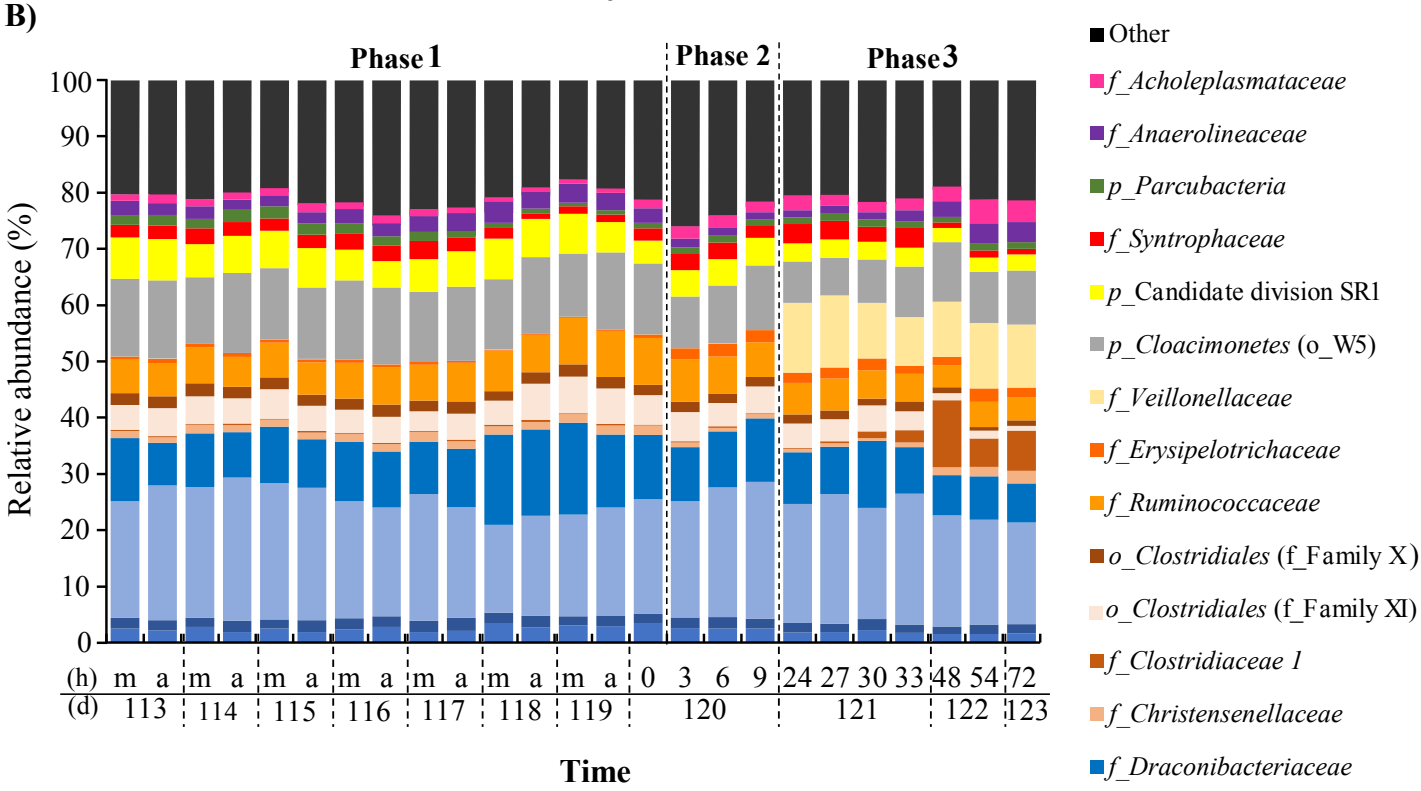
B)
Phase 1
Phase 2
Phase 3
Relative abundance (%)
100
90
80
70
60
50
40
30
20
10
0
(h) m a m a m a m a m a m a m a 0 3 6 9 24 27 30 33 48 54 72
(d) 113 114 115 116 117 118 119 120 121 122 123
Time
Other
f_Acholeplasmataceae
f_Anaerolineaceae
p_Parcubacteria
f_Syntrophaceae
p_Candidate division SR1
p_Cloacimonetes (o_W5)
f_Veillonellaceae
f_Erysipelotrichaceae
f_Ruminococcaceae
o_Clostridiales (f_Family X)
o_Clostridiales (f_Family XI)
f_Clostridiaceae 1
f_Christensenellaceae
f_Draconibacteriaceae

Fig5

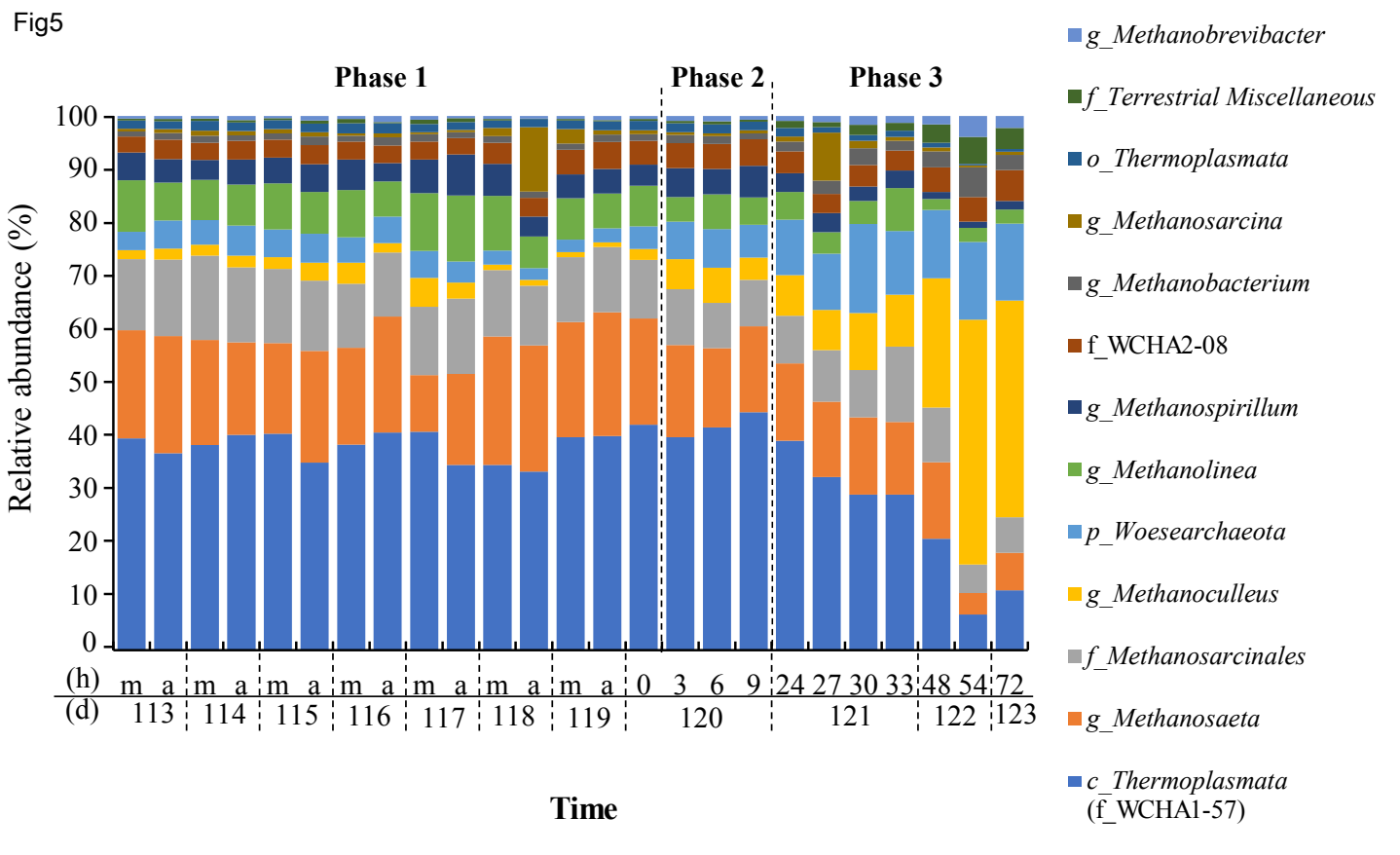
Phase 1
Phase 2
Phase 3
Relative abundance (%)
100
90
80
70
60
50
40
30
20
10
0
(h) m a m a m a m a m a m a m a 0 3 6 9 24 27 30 33 48 54 72
(d) 113 114 115 116 117 118 119 120 121 122 123
Time
g_Methanobrevibacter
f_Terrestrial Miscellaneous
o_Thermoplasmata
g_Methanosarcina
g_Methanobacterium
f_WCHA2-08
g_Methanospirillum
g_Methanolinea
p_Woesearchaeota
g_Methanoculleus
f_Methanosarcinales
g_Methanosaeta
c_Thermoplasmata (f_WCHA1-57)

Fig6

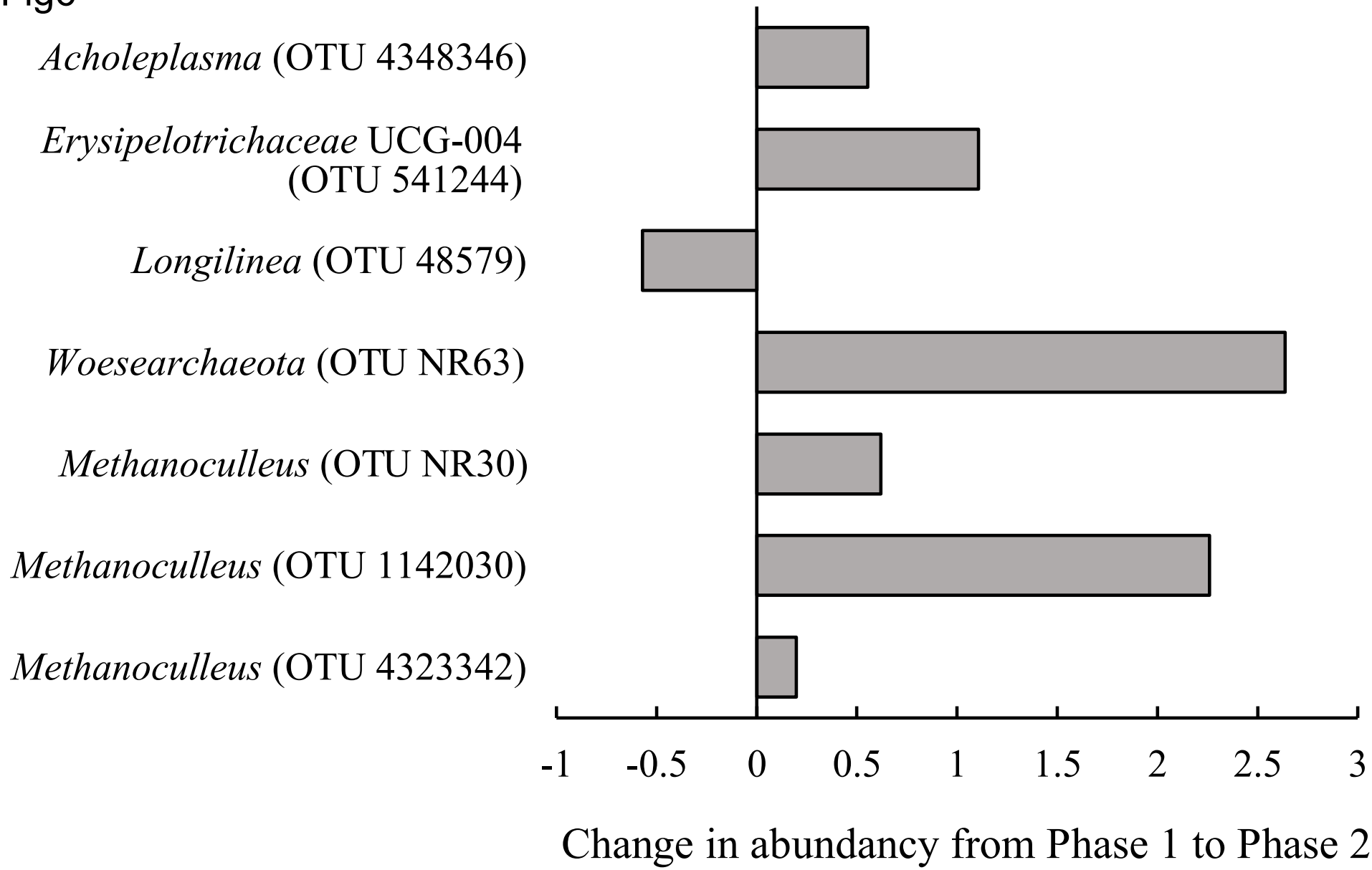
Acholeplasma (OTU 4348346)
Erysipelotrichaceae UCG-004 (OTU 541244)
Longilinea (OTU 48579)
Woesearchaeota (OTU NR63)
Methanoculleus (OTU NR30)
Methanoculleus (OTU 1142030)
Methanoculleus (OTU 4323342)
-1
-0.5
0
0.5
1
1.5
2
2.5
3
Change in abundancy from Phase 1 to Phase 2

Fig7

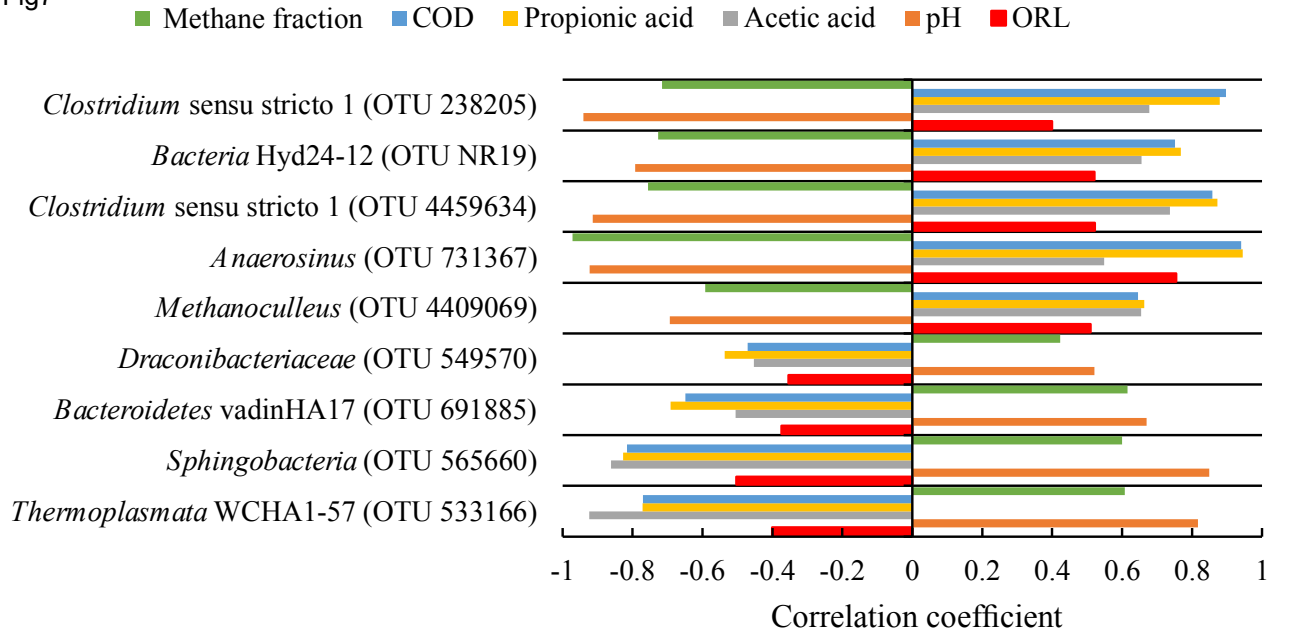
Methane fraction
COD
Propionic acid
Acetic acid
pH
ORL
Clostridium sensu stricto 1 (OTU 238205)
Bacteria Hyd24-12 (OTU NR19)
Clostridium sensu stricto 1 (OTU 4459634)
Anaerosinus (OTU 731367)
Methanoculleus (OTU 4409069)
Draconibacteriaceae (OTU 549570)
Bacteroidetes vadinHA17 (OTU 691885)
Sphingobacteria (OTU 565660)
Thermoplasmata WCHA1-57 (OTU 533166)
-1
-0.8
-0.6
-0.4
-0.2
0
0.2
0.4
0.6
0.8
1
Correlation coefficient